A Design of Four-Port Flexible UWB-MIMO Antenna for Wearable and IoT Applications

Jia Wei Tan[1], Sew Sun Tiang[1, *], Kim Soon Choong[1], Mohammad Arif Bin Ilyas[1], Mastaneh Mokayef[1], Zhi Ying Yeoh[1], Wei Kang Lai[1], Wei Hong Lim[1]

E-mail: 1001954282@ucsiuniversity.edu.my, tiangss@ucsiuniversity.edu.my, ChongKS@ucsiuniversity.edu.my, mohammadarif@ucsiuniversity.edu.my, mastaneh@ucsiuniversity.edu.my, 1001953809@ucsiuniversity.edu.my, 100953677@ucsiuniversity.edu.my, limwh@ucsiuniversity.edu.my

([1]UCSI University, Malaysia)

** Corresponding author*

Abstract

This paper introduces a compact four-port MIMO antenna for ultrawideband (UWB) applications measuring 60 × 60 mm^2. Printed on a single layer flame resistant (FR-4) substrate (permittivity of 4.3, thickness 1.6mm), the antenna features four microstrip cells, each orthogonal to its neighbor for improved isolation. It includes a rectangular patch with staircase slits and a stepped feed line. Square stubs at the top center enhance isolation. The antenna boasts a significant return loss (-43.75dB), wide impedance bandwidth (1.967-12GHz), and an isolation below -15dB. Its envelope correction coefficient (ECC) is under 0.02 with a moderate 4.4dBi gain. Although its 63% radiation efficiency could be enhanced, the antenna's ultrawide bandwidth and compactness make it suitable for UWB wearable IOT applications.

Keywords: UWB antenna, MIMO antenna, MIMO performance.

1. Introduction

The frequency of ultra-wideband (UWB) technology was set to 3.2-10.6GHz by the Federal Communication Commission (FCC) which garnered great attention of researchers due to its promising solution to scarcity of spectrum resources. Compared to traditional narrowband technology, UWB offers more advantages and several capabilities including short range, high transmission, high bandwidth, low energy usage, low complexity, and good radiation. With this, UWB positions itself to being useful in applications such as short-range communications, sensor networks, tracking, and positioning systems [1], [2].

In a multi-path environment, UWB systems are prone to signal fading which degrades the performance of the entire system. To address this issue, Multi-Input-Multi-Output (MIMO) technology has been used to provide a multi-element patch antenna for signal transmission and reception. This implementation significantly increases spectral efficiency, reliability, and channel capacity without utilizing additional power and spectrum. The enhanced features of MIMO UWB antennas such as high data rate and exclusion from interference make it a perfect candidate for wearable and IoT applications especially in healthcare industries. Radiation exposure from the antenna is heavily monitored to be as small as possible to ensure that it does not harm human tissues since it is in close contact with human skin [2].

However, the usage of more than one radiating element, closely arranged to one another in MIMO may lead to high signal correlation and reduce the overall antenna efficiency. Therefore, appropriate decoupling needs to be done between antenna elements for better isolation in modern communication. The challenging part is to design UWB-MIMO with low isolation by keeping minimum distance between antennas. In [1], a UWB-MIMO antenna with square shaped decoupler and rectangular metallic stubs was designed to reduce mutual coupling and improve isolation. The antenna offers stable gain with peak gain at 6.8dBi, low ECC value of 0.001 and high diversity gain of 9.9. Besides, flexible substrates such as polymer, paper, and Kapton are important in the designing of wearable UWB. In [3], a wristband MIMO antenna is designed that covers frequency range of 2.75-12GHz with silicone rubber as substrate material that is used to monitor children and patients, ensuring user safety. In [4], the author proposed the use of liquid crystal polymer (LCP) that operates between 2.9-10.86GHz which results in a flexible MIMO antenna that performs well in bending and on-body conditions, suitable in wearable fields. Another result obtained from [5], uses bendable substrate FR-4 that operates up to 17GHz from 3.89GHz with stable gain.

Moreover, the design of UWB is very challenging to achieve optimized frequency and time, stable polarization, as well as low dispersion. In [6], the author proposed a methodology that introduces slotted ground structure which is a widely used technique to improve the impedance bandwidth and minimize the ground plane effects in UWB. In [7], 4 ports rectangular monopole antennas with step etching on ground plane and arrow-shaped slot on radiating patch using FR-4 substrate operates at frequency 3.1-10.6GHz, has high isolation of -17.4dB, ECC less than 0.001 which in turn decreases mutual coupling. In the medical field, wearable devices are achieving profound recognition when designed using MIMO antenna due to their quality signal and high capacity without increasing transmitted power.

This paper proposes the design of four port UWB-MIMO antenna suitable for wearable and IoT applications which is done by utilizing the CST software that involves careful selection of flexible substrate properties, structure of microstrip patch, and feed network. The design uses copper conductor for patch and FR-4 as substrate material that covers wider bandwidth and higher efficiency characteristic with low dielectric loss and high thermal endurance. The width of the microstrip and gap between the patches are adjusted to obtained impedance matching of 50 Ohm. The finalized antenna is measured at different parameters such as reflection coefficients, gain, radiation pattern, current distribution, ECC, DG, radiation and total efficiency for further analysis and improvements. Table1 shows summary of comparison between existing UWB-MIMO antennas and proposed work.

Table 1. Summary Of Comparison Between Existing UWB-MIMO Antennas and Proposed Work

References	**Operating Frequency (GHz)**	**Peak Gain (dBi)**	**Dimension (mm^3)**	**Envelope Coefficient Correlation (ECC)**	**Diversity Gain (DG)**	**Isolation (dB)**	**Substrate Type**
[3]	2.75-12.0	3.41	24 × 30 × 0.13	< 0.18	> 9.5	> 25	Silicon Rubber
[4]	2.90-10.86	4	65× 65 × 0.1	< 0.01	> 9.99	> 22	Liquid Crystal Polymer (LCP)
[5]	3.89-17.09	5.87	75 × 91 × 0.26	< 0.02	-	> 22	FR-4
[6]	2.9-12.4	3.09	30 ×30 × 1.6	-	-	-	FR-4
[7]	2.6-11	3.38	80 × 80 × 0.781	< 0.001	-	-17.4	FR-4
[8]	3.6-16.00	7	58× 58 × 0.8	< 0.07	-	> 18	FR4
[9]	1.5-3.6	2.4	26× 26 × 0.8	< 0.02	> 9.9	~ 25	FR4
[10]	3.3-13.6	5.7	42 × 32.5 × 1.0	< 0.02	> 9.96	> 18	Textile
[11]	3.10-12	6.2	30× 30 × 1.6	< 0.001	> 9.9	~ 17	FR-4
[12]	3.1-13.1	4	45 × 45 × 1.6	< 0.02	> 9.9985	< 17	FR-4
[13]	3.5-11	6	24 × 30 × 0.13	< 0.03	> 9.9	< 20	FR-4
Proposed work	1.926-12	4.409	60 × 30 × 1.187	<0.02	>9.93	>15	FR-4

2. Material and Methods

2.1 Single Element Antenna Design

The configuration of the proposed UWB single element microstrip antenna shown in Fig. 1. The fundamental structure of the antenna consists of three layers which are metal layer on top and bottom with substrate material, in between. The design begins with a rectangular radiating patch that uses a 50Ohm transmission line feeding technique to feed signal to the resonating patch. The ground plane size is decreased for low profile and optimization for attaining enhanced impedance bandwidth. Two symmetrical staircase-shaped slits are introduced on both sides of the radiating patch to further enhance the impedance bandwidth.

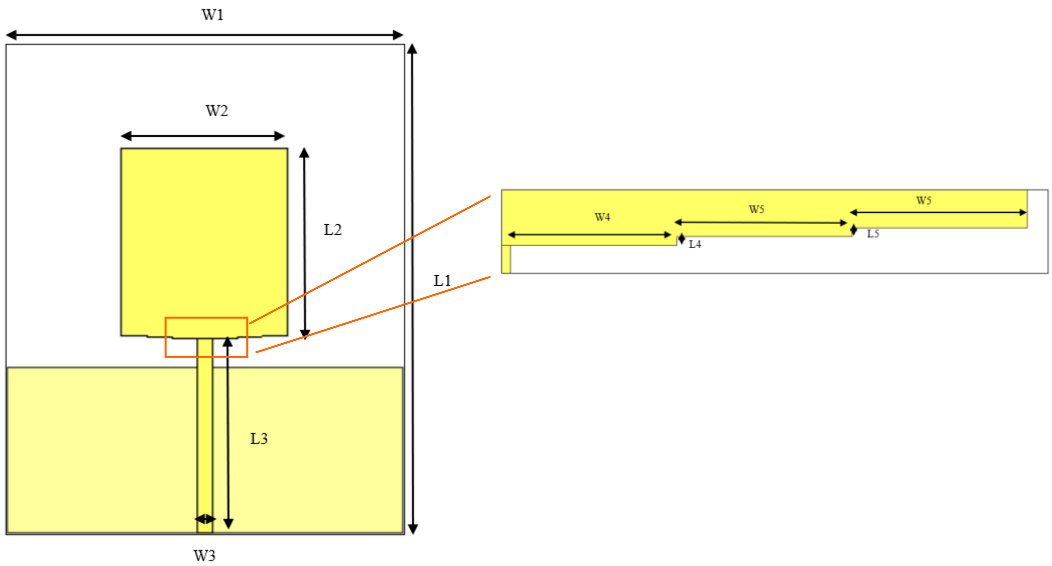

a. Front view of antenna design b. Magnified area for staircase-like slits

Fig. 1 Geometry of proposed antenna design.

Table 2. Optimized Parameters for the Proposed Four Port MIMO Antenna.

Parameters	W1	W2	W3	W4	W5
Values (mm)	31	13	3	1.65	2
Parameters	L1	L2	L3	L4	L5
Values (mm)	42	15.6	15.3	0.1	13

Table 2 shows the optimized parameters for the proposed four port MIMO antenna. The material chosen for the antenna patch is copper (annealed) because it is much softer and malleable which makes it easier to shape during the fabrication stage. On the other hand, the flexible dielectric substance used is flame-resistant (FR4) with dielectric constant of 4.3 and tangent loss of 0.019. Some key features of this substrate material include low cost, easily available and relative mechanical and electrical stability. It is mostly found in microstrip and stripline circuits, as well as point-to-point digital radio antennas. The thickness of the UWB microstrip antenna is 1.8mm with copper (annealed) 0.1mm and substrate as 1.6mm respectively. Overall, the FR4 substrate based UWB antenna, and its resonating patch has sizes of $31 \times 42 \times 1.7$ mm^3 and fed by a $3 \times 17 \times 0.1$ mm^3 transmission line.

The operating range of antenna generated is 2.74-10.59GHz shown in Fig. 2 which fulfills the requirement of UWB but is lesser compared to the values from the article [14] which obtain 2.9-11GHz.

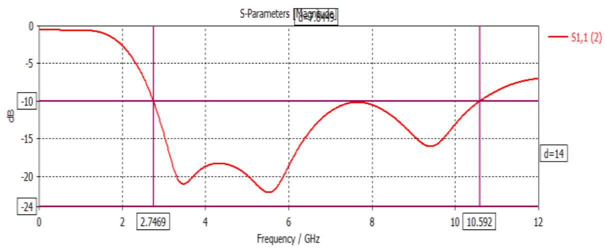

Fig. 2 Simulation results of return loss (S11) for single-slot antenna

2.2 Four-Element Flexible UWB Antenna

From the single element in Fig. 1, a four-port flexible MIMO antenna array was designed as shown in Fig. 3 (b) with a square-shaped stub inserted between orthogonal element antennas for better isolation performance.

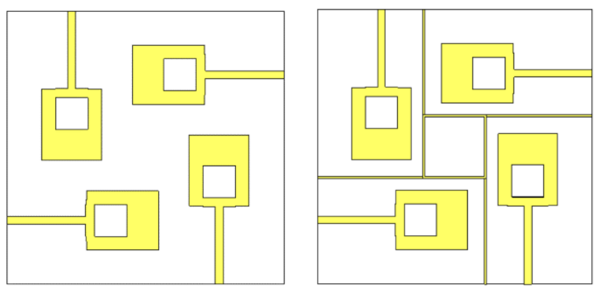

a. Without isolator b. With isolator branch

Fig 3. Four Port UWB MIMO antenna

3. Result and Discussion

The layouts were designed and simulated using CST software to determine the antenna performance in different aspects.

The S11 parameter graph is a measure of how well devices or lines are matched. A high return loss is desirable for lower insertion loss. The simulated result for return loss from the proposed UWB four-port antenna is displayed in Fig. 4 (a). The first antenna result without branch isolator (green line) shows much narrow impedance bandwidth with frequency range of 3.925-12GHz for S11 < -10dB. Besides, the return loss value is acceptable, which is -22.49dB at resonant frequency of 4.42GHz but can be improved to reduce power reflected to the system. This leads to the addition of a branch isolator (red line) to improve both return loss and bandwidth values. The S11 value almost increased twofold with value highest return loss value of -43.94dB at resonant frequency of 8.124GHz, larger bandwidth, and wider frequency range of 1.926-12GHz. The rest of the resonant frequencies for S11 below -10dB are recorded at 2.292GHz, 4.14GHz, 6.6GHz and 11.076GHz.

The remaining parameters are also compared such as S12, S13 and S14 to determine the isolation as shown in Fig 4 (b), (c), (d). The measured operating frequency covers 2.0-12GHz. The implementation of branch isolators affects S12, S13, and S14 whereby most of them are below -15dB (red line) and this shows good isolation properties. With an almost similar isolation design, the result from A. A. Ibrahim, et al [13] shows better isolation which is greater than -20dB when the isolation ports are added.

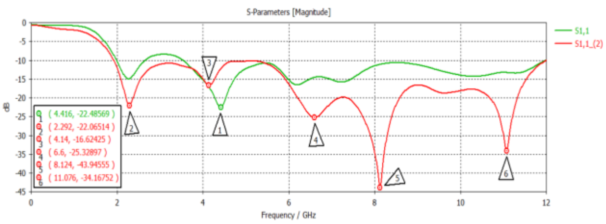

(a) S11

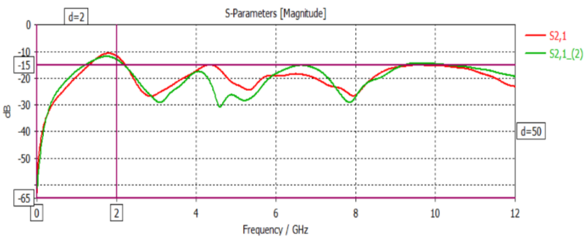

(b) S12

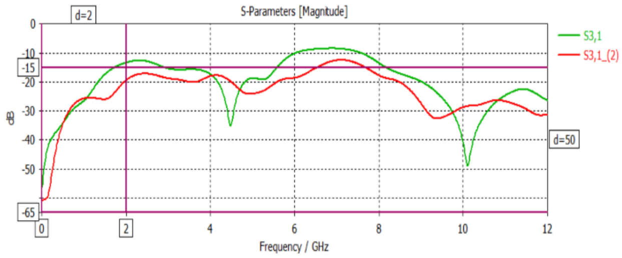

(c) S13

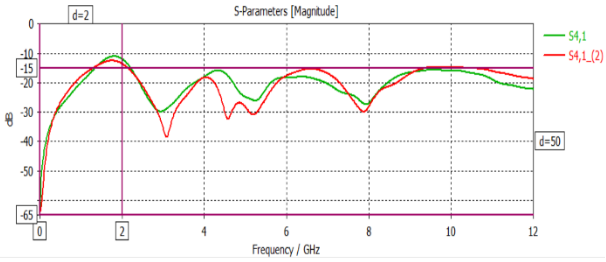

(d) S14

Fig 4. Results of return loss and isolation loss

The gain and directivity for the final proposed antenna on different resonant frequencies is tabulated in Table 3 while the far field pattern for resonant frequency, 8.124GHz is shown in Fig. 5 (a) and (b).

Table 3. Gain and Directivity Values for Different Resonant Frequencies

Resonant Frequency (GHz)	Gain (dBi)	Directivity (dBi)
2.292	4.407	6.36
4.14		
6.6		
8.124		
11.076		

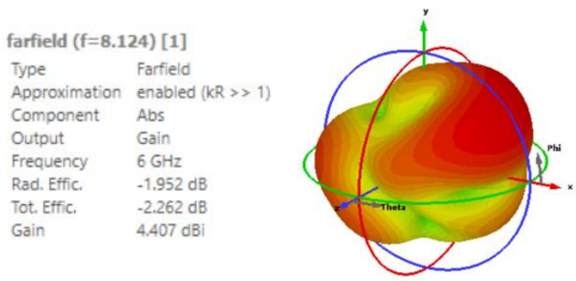

(a) Gain at resonant frequency of 8.12GHz.

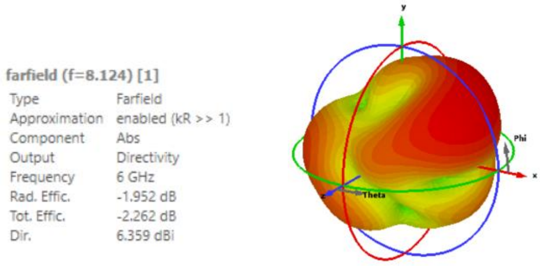

(b) Directivity at resonant frequency of 8.124GHz.

Fig 5. Gain and directivity at resonant frequency of 8.124GHz.

Fig. 6 (a), Fig. 6(b), Fig. 6(c), Fig. 6(d), and Fig. 6(e) shows the radiation pattern of the proposed four-port flexible antenna on H-plane and E-plane at different resonant frequencies. The simulation and test results were obtained when port 1 was used as excitation. The H-field and E-field exhibit a directional pattern whereby the energy is concentrated and focused on specific directions at degrees of 44° and 178° for all resonant frequencies. It allows far-distance communication due to higher gain and directivity.

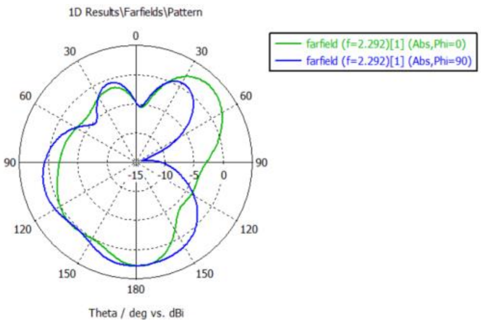

(a) Radiation pattern at 2.292GHz.

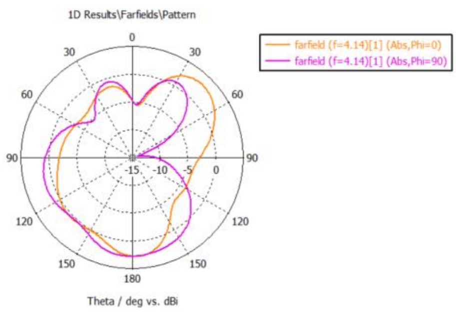

(b) Radiation pattern at 4.414GHz.

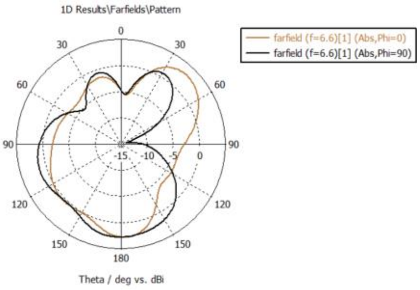

(c) Radiation pattern at 6.6GHz.

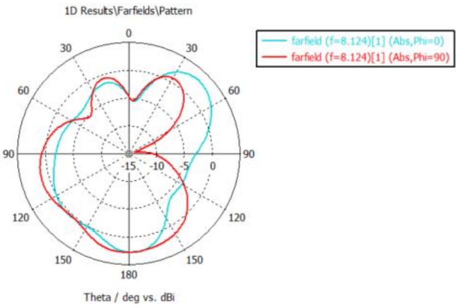

(d) Radiation pattern at 8.124GHz.

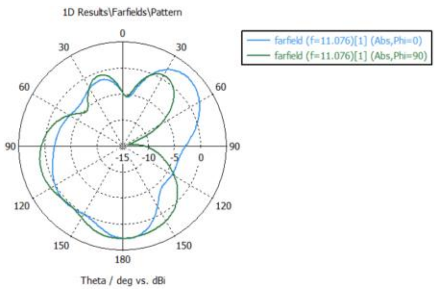

(e) Radiation pattern at 11.076GHz.

Fig 6. Radiation pattern on H-plane and E-plane of four port MIMO UWB antenna at different resonant frequencies

The surface current distribution is measured at port 1, 2, 3 and 4 with resonant frequencies at 2.292GHz, 4.14GHz, 6.6GHz, 8.124GHz and 11.076GHz and tabulated in Table 4. Fig. 7 shows the pattern of the selected resonant frequency, 8.124GHz, where the rest have similar current diagrams. The current density is most evident at the antenna feedline denoted by warm colors of red and orange color map which contributes to stronger radiation and better performance but can result in higher potential for losses and prone to heating easily due to high dissipation of electromagnetic fields and energy. The rest of the areas that are mostly displayed in blue or green colors experience low current density whereby it has weaker radiation and signal strength but less susceptible to losses.

Table 4. Surface Current Value at Port 1 to 4 at Different Resonant Frequencies.

<table>
<tr><th>Resonant Frequency (GHz)</th><th>Port 1 (A/m)</th><th>Port 2 (A/m)</th><th>Port 3 (A/m)</th><th>Port 4 (A/m)</th></tr>
<tr><td>2.292</td><td rowspan="3">37.0092</td><td rowspan="3">37.9358</td><td rowspan="3">38.3408</td><td rowspan="3">37.0869</td></tr>
<tr><td>4.14</td></tr>
<tr><td>6.6</td></tr>
<tr><td>8.124</td><td>29.5007</td><td>33.4613</td><td>30.3317</td><td>34.7738</td></tr>
<tr><td>11.076</td><td>37.0092</td><td>37.9358</td><td>38.3408</td><td>37.0869</td></tr>
</table>

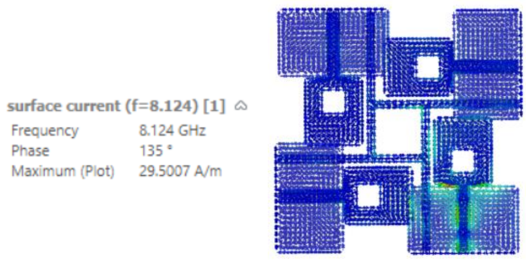

Fig. 7 Surface current distribution of four-port UWB MIMO antenna at resonant frequency, 8.124GHz.

The average radiation and total efficiency of the antenna is only recorded between 6GHz-12GHz due to mesh limitation in frequency domain. Fig. 8 shows the value in dB (magnitude) which is approximately 55% and 54% after converted to percentage form. These values are considered marginally acceptable because good antenna design can reach up to 80%. Hence, the design can still be further improved by careful calculation of geometry and dimensions, matching networks to achieve maximum performance whereby it provides better signal strength and reduces interference which are important factors for improving the reliability and operability of wearable devices in IoT applications.

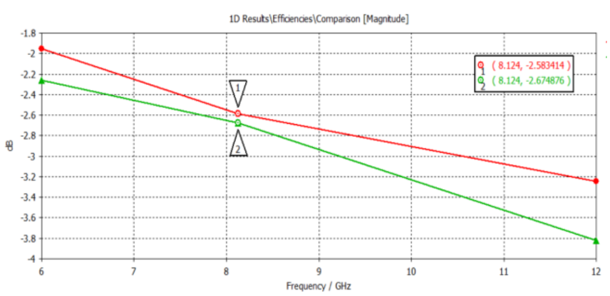

Fig. 8 Radiation efficiency and total efficiency of four-port UWB MIMO antenna.

The diversity performance of the UWB-MIMO antenna was evaluated by Envelope Coefficient Correlation (ECC) and diversity gain (DG). ECC parameters reflect the degree of correlation between adjacent elements of MIMO antennas and are expected to be less than 0.5. The ECC parameters between the antenna's ports are shown in Fig. 9 (a) which are less than 0.02 in the operating frequency band and indicate good isolation between ports.

DG evaluates the quantified improvement in signal-to-noise ratio when antenna in the MIMO system receive the RF signal. The DG parameters between different ports are given in Fig. 9 (b) It shows that satisfying DG values are achieved with values above 9.938 for the whole operating frequency band (1.926-12GHz) which gives better diversity characteristics.

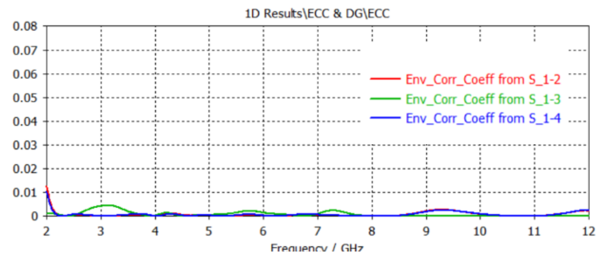

(a) ECC

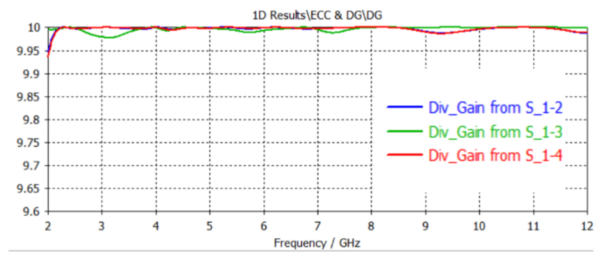

(b) DG

Fig 9. ECC and DG values for four-port UWB MIMO antenna.

Conclusion

This paper proposed a small, compact, and flexible four-port UWB MIMO antenna designed for wearable and IoT applications with overall dimensions of $60 \times 60 \times 1.8$ mm^3. The proposed antenna was arranged orthogonally to each other to form a four-port MIMO antenna structure and the final design shows that the antenna can operate in the whole UWB band covering from 1.926 to 12GHz with moderate isolation of -15dB. The isolation was achieved by adding a square-shaped stub at the top center with elongated strips extending to the edge of the substrate. It has a high return loss value of -43.65dB, total efficiency of approximately 60%, gain of 4.4dBi, and good diversity performance, with ECC less than 0.02 and DG larger than 9.93dB. In summary, the proposed antenna can be considered as a viable candidate for UWB-MIMO wireless applications.

Acknowledgements

This work was supported by the UCSI University Research Excellence & Innovation Grant (REIG) with project code of REIG-FETBE-2022/038.

References

1. Abbas, N. Hussain, M. A. Sufian, J. Jung, S. M. Park, and N. Kim, "Isolation and gain improvement of a rectangular notch uwb-mimo antenna," *Sensors*, vol. 22, no. 4, Feb. 2022.
2. P. Kumar, P. Kumar, T. Ali, P. Kumar, and S. Vincent, "Ultrawideband Antennas: Growth and Evolution," *Micromachines*, vol. 13, no. 1. MDPI, Jan. 01, 2022.
3. T. Govindan *et al.*, "On the design and performance analysis of wristband MIMO/diversity antenna for smart wearable communication applications," *Sci Rep*, vol. 11, no. 1, Dec. 2021.
4. J. Zhang, C. Du, and R. Wang, "Design of a Four-Port Flexible UWB-MIMO Antenna with High Isolation for Wearable and IoT Applications," *Micromachines (Basel)*, vol. 13, no. 12, Dec. 2022.
5. Desai, J. Kulkarni, M. M. Kamruzzaman, S. Hubalovsky, H. T. Hsu, and A. A. Ibrahim, "Interconnected CPW Fed Flexible 4-Port MIMO Antenna for UWB, X, and Ku Band Applications," *IEEE Access*, vol. 10, pp. 57641–57654, 2022.
6. T. Ali and R. C. Biradar, "A Miniaturized Volkswagen Logo UWB Antenna with Slotted Ground Structure and Metamaterial for GPS, WiMAX and WLAN Applications," 2017.
7. W. Naktong and A. Ruengwaree, "Four-Port Rectangular Monopole Antenna for UWB-MIMO Applications," 2020.
8. P. Kumar, S. Urooj, and F. Alrowais, "Design and implementation of quad-port MIMO antenna with dual-band elimination characteristics for ultra-wideband applications," *Applied Sciences (Switzerland)*, vol. 10, no. 5, Mar. 2020.
9. I. Elfergani *et al.*, "Low-profile and closely spaced four-element mimo antenna for wireless body area networks," *Electronics (Switzerland)*, vol. 9, no. 2, Feb. 2020.
10. S. Kumar *et al.*, "Wideband Circularly Polarized Textile MIMO Antenna for Wearable Applications," *IEEE Access*, vol. 9, pp. 108601–108613, 2021.
11. A. H. Jabire, S. Sani, S. Saminu, M. J. Adamu, and M. I. Hussein, "A crossed-polarized four port MIMO antenna for UWB communication," *Heliyon*, vol. 9, no. 1, Jan. 2023.
12. A. Wu, M. Zhao, P. Zhang, and Z. Zhang, "A Compact Four-Port MIMO Antenna for UWB Applications," *Sensors*, vol. 22, no. 15, Aug. 2022.
13. A. A. Ibrahim, M. I. Ahmed, and M. F. Ahmed, "A systematic investigation of four ports MIMO antenna depending on flexible material for UWB networks," *Sci Rep*, vol. 12, no. 1, Dec. 2022.
14. M. Mustaqim, B. A. Khawaja, H. T. Chattha, K. Shafique, M. J. Zafar, and M. Jamil, "Ultra-wideband antenna for wearable Internet of Things devices and wireless body area network applications," *International Journal of Numerical Modelling: Electronic Networks, Devices and Fields*, vol 32, no.6 Nov. 2019.

Authors Introduction

Ms. Jia Wei Tan

She is currently pursuing Bachelor of Engineering Communication and Electronics with Honors as final year student in Faculty of Engineering, Technology and Built Environment, UCSI University, Malaysia. Her research interests are communication and antenna design.

Dr. Sew Sun Tiang

She is an Assistant Professor in Faculty of Engineering at UCSI University in Malaysia. She received her PhD in Electrical and Electronic Engineering from Universiti Sains Malaysia in 2014. Her research interests are optimization and antenna design.

Dr. Kim Soon Choong

He obtained his B.Eng., M.S., and Ph.D. degrees in electrical and electronic engineering from Universiti Kebangsaan Malaysia in 2012, 2015, and 2019, respectively. He currently serves as an Assistant Professor in the Department of Computer Engineering (Artificial Intelligence) within the Faculty of Engineering Technology and Built Environment at UCSI Kuala Lumpur. His research focuses on areas such as medical signal processing and instrumentation.

Dr. Mohammad Arif Bin Ilyas

He (M'32) was born in Malaysia in 1991. He received his PhD in Electrical Engineering from Universiti Tun Hussein Onn Malaysia in 2020. He also earned his bachelor's degree in electronic engineering at the same university. Currently, he is a lecturer in the Faculty of Engineering, Technology, and Built Environment at UCSI University. His main areas of research interest are machine learning, artificial intelligence, the Internet of Things, embedded systems, and optical wireless communication, especially visible light communication.

Dr. Mastaneh Mokayef

She has received her PhD from Wireless Communication Centre Faculty of Electrical Engineering in University Technology Malaysia (UTM) in 2014. She has also obtained her master's degree from the faculty of engineering in 2009 from the University Technology Malaysia. Her research interests include Wireless communications, spectrum sharing method, spectrum management, cellular communication systems and Antenna design.

Ms. Zhi Ying Yeoh

She is currently pursuing Bachelor of Engineering Electrical and Electronics with Honours as final year student in Faculty of Engineering, Technology and Built Environment, UCSI University, Malaysia. Her research interests are power electronics and simulation.

Mr. Wei Kang Lai

He is currently pursuing Bachelor of Electrical and Electronics Engineering as final year student in Faculty of Engineering, Technology and Build Environment, UCSI University, Malaysia. His research interests are electrical and solar system design.

Dr. Wei Hong Lim

He is an Assistant Professor in Faculty of Engineering at UCSI University in Malaysia. He received his PhD in Computational Intelligence from Universiti Sains Malaysia in 2014. His research interests are optimization and artificial intelligence.